Magnetic-field-induced alignment-to-orientation conversion in sodium

X. L. Han* and G. W. Schinn†
Joint Institute for Laboratory Astrophysics, National Institute of Standards and Technology and University of Colorado, Boulder, Colorado 80309-0440
(Received 23 July 1990)

We report a detailed investigation of excited-state alignment-to-orientation conversion in the presence of an external magnetic field. This counterintuitive phenomenon occurs under intermediate-coupling conditions. A weak, linearly polarized, cw laser beam was used to excite and align the Na $3P_{3/2}$ state in an atomic beam along the z direction. The degree of circular polarization of the resulting fluorescence was detected along the z direction as a function of magnetic-field strength. The spectrally integrated transitions originating from individual F levels of the $3S_{1/2}$ state yield a maximum circular-polarization fraction of $\sim 40\%$; integrating the circular polarization over all the allowed $3S_{1/2}$-$3P_{3/2}$ transitions gives rise to an $\sim 8\%$ effect. The results are predicted by the Breit formula, which is in excellent agreement with our observations.

I. INTRODUCTION

In an aligned atomic system, states of different $|m_L|$ are populated unequally, while the populations in m_L and $-m_L$ are the same. In contrast, an oriented system is characterized by differing populations in the m_L and $-m_L$ states. A necessary condition for the production of an aligned exited state is that the excitation process be anisotropic. The direct production of an oriented excited state from an unoriented ground state requires an orientation or polarization of the exciting particles (e.g., photons, electrons, etc.).

Internal interactions within the excited atom, such as fine- and hyperfine-structure coupling, occur on a time scale generally much longer than the ($\sim 10^{-15}$ s) time required for collisional or incoherent optical excitation, and much less than the ($\sim 10^{-8}$ s) radiative decay time of the state.

Conversion of the excited-state alignment into orientation can occur during the time between excitation and decay. As shown by Fano and Macek,[1] this cannot result from internal interactions alone, but can take place if these interactions are combined with the action of an external magnetic field.

Alignment-to-orientation conversion (AOC) was first discussed in the context of a nuclear spin $I=\frac{1}{2}$ system by Lehmann,[2] who later experimentally verified that ^{111}Cd could be given a net orientation using broadband, linearly polarized light excitation. Baylis[3] described this effect in sodium, and discussed its relevance to level-crossing signals. Kemp, Macek, and Nehring[4] presented a comprehensive theoretical discussion of AOC processes. They noted this effect may be responsible for the small net circular polarization observed in light emission from sunspots.

The first experiment to directly detect a net circular polarization of the fluorescence from an initially aligned excited state was reported by Krainska-Miszczak.[5] In that work, linearly polarized light from a Rb-Ar lamp was used to excite the ^{85}Rb $5S_{1/2}$-$5P_{3/2}$ transition, and the subsequent fluorescence observed along the magnetic-field direction. The resulting hyperfine-structure-induced AOC was in good qualitative agreement with theory.

More recently, AOC effects in the aligned $(1s3d)^3D$ state of He have been the subject of some controversy. Stricklett, Burns, and Burrow[6] first reported confirmation of fine-structure-induced AOC in this electron-excited system, but these results were called into question in a subsequent publication by Avci and Neitzke.[7] This latter group reported good agreement with theory for results of their own experiment using He^+ projectiles to excite this same ^3D state. They report circular-polarization fractions measured at five magnetic-field strengths ranging up to 200 G (where a 3.7% effect was seen), but experimental limitations kept their results well below the ~ 600 G at which the AOC in this system should have a maximum effect.

We report here measurements and calculations of hyperfine-interaction-induced AOC in Na, for a magnetic-field range that shows the full coupling dependence of this process. The nearly monochromatic nature of our exciting laser yields much more information than can be extracted from collisional or equivalent broadband optical excitation, since it allows us to isolate the large effects occurring for excitation from single ground F states. Moreover, the laser intensity is monitored as a function of frequency, allowing accurate results to be obtained. This is in contrast with the experiment of Ref. 5, where only qualitative effects could be measured, on account of the uncertainty in the lamp's excitation profile.

Optical excitation is highly efficient on the Na first-resonance ($3S$-$3P$) transition, due to its large oscillator strength and its experimentally favorable (590-nm) wavelength, which renders it an excellent candidate for this study. As a consequence, our absolute signal levels are much better than those from the above-mentioned He experiments, which were hampered by the inherently much lower charged-particle excitation probabilities.

II. THEORY

AOC may seem at first to be a very surprising phenomenon. Consider an ensemble of atoms excited to the $m_L=0$ sublevel of an $L=1$ state at $t=0$, i.e., the atoms are aligned. For simplicity, assume that there is no net nuclear spin and hence no hyperfine structure. If there is a nonzero electronic spin, then the spin-orbit and magnetic-field interactions will cause excited atoms to partially evolve into $m_L=1$ and $m_L=-1$ states before radiative decay. Intuitively, one might expect the net population of the $m_L=\pm 1$ state to be equal, and indeed, for very small or very large magnetic fields these populations are essentially the same, i.e., alignment normally is not converted into orientation. However, when the magnetic-field strength is such that the states are in intermediate coupling, the populations of $m_L=1$ and $m_L=-1$ become different; alignment-to-orientation conversion occurs.

Semiclassically, AOC may be regarded as taking place because of the different precession speeds of the spin and orbital angular momenta in the presence of an external magnetic field.[4] Consider an ensemble of atoms, each having electronic spin $S=\frac{1}{2}$ and orbital angular momentum $L=1$. In the absence of the magnetic field, **L** is coupled to **S**, giving **J**, which is a good quantum number, and **S** and **L** precess about **J** with a frequency corresponding to the fine-structure splitting. If the initially unexcited atoms have equal populations in $m_S=\pm\frac{1}{2}$, and are excited by light polarized along the **z** direction, an excited $m_L=0$ state will result. If the **L** and **S** are coupled to form J, m_J states, then $\langle L_z\rangle=0$, i.e., no orientation is produced. Now, in the presence of magnetic field, **S** and **L** not only try to precess about **J** together, but also attempt to separately precess about the magnetic field. Since the ratio of gyromagnetic constants, g_S/g_L is two, precession about the external field occurs at different rates for **S** and **L**, leading to a change in $\langle L_z\rangle$, i.e., a partial conversion of alignment to orientation.

For atoms with hyperfine structure, the above arguments carry over to the partial decoupling of total angular momentum **F** into **I** and **J**. The sodium $3P_{3/2}$ state exhibits a transition region for **I**·**J** decoupling at ~ 40 G, whereas that for **L**·**S** coupling is found at nearly 100 kG. For reasons of experimental convenience, it is AOC arising from hyperfine decoupling which is studied here.

Quantum mechanically, this AOC process may be viewed as resulting from the interference of different excitation-decay pathways, as the energy levels of differing magnetic sublevels cross in the presence of an external magnetic field. When the distance between any two curves is less than the lifetime-broadened width of the states, interference can occur. This is described analytically using the Breit formula, which gives the rate $R(\mathbf{f},\mathbf{g})$ at which white-light photons of polarization **f** are absorbed and photons of polarization **g** are reemitted:[8]

$$R(\mathbf{f},\mathbf{g})=c\sum_{\alpha,\beta,i,j}\frac{f_{i\alpha}f_{\alpha j}g_{j\beta}g_{\beta i}}{1-2\pi i\tau\nu_{ij}}\ . \tag{1}$$

In this expression, $f_{i\alpha}$ is the appropriate electric-dipole matrix element ($=\langle i|\mathbf{f}\cdot\mathbf{r}|\alpha\rangle$), τ is the mean lifetime of each excited state, ν_{ij} is the separation between excited-state sublevels i and j in frequency units, α and β are ground-state sublevels, and c is a constant incorporating the photon intensity, geometric factors, etc. Franken[8] has shown that this result holds independently of whether the white light is coherent (e.g., a short pulse) or incoherent. A similar formula exists for monochromatic excitation,[9] which one could evaluate and then average over the residual beam Doppler spread for comparison to the single-frequency data, such as that shown in Fig. 3. However, this would require considerable additional effort, and we have no reason to expect any differences in the final result, particularly since the spectrally integrated data yield excellent agreement with the Breit formula. Thus, this has not been done here.

Figure 1 shows an energy diagram for the $3P_{3/2}$ magnetic sublevels as a function of magnetic-field strength from 0 to 100 G. At zero field the spacings are due to the hyperfine interaction and the states are well described in the F, m_F representation; at 100 G they are essentially recoupled into the m_J,m_I representation. This level structure was calculated in the standard fashion by di-

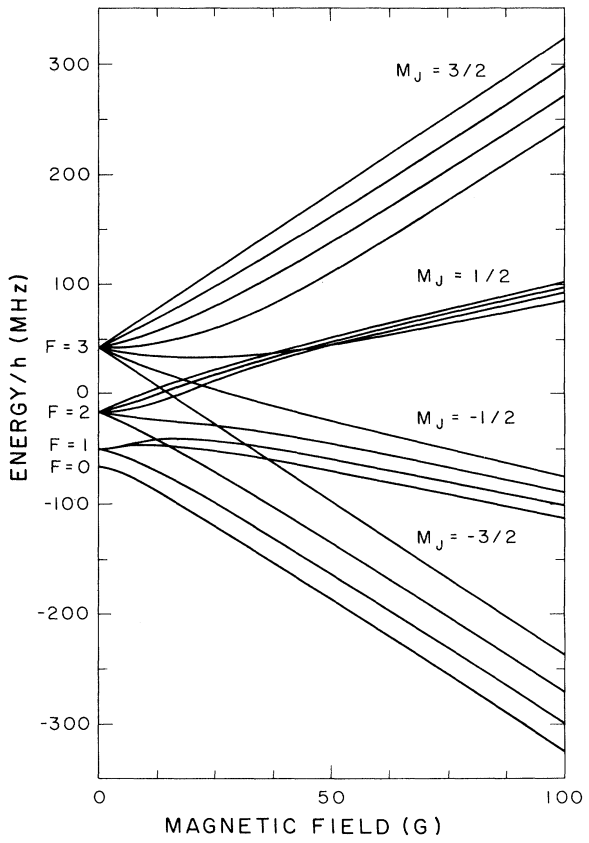

FIG. 1. Magnetic-field dependence of the 16 sublevels comprising the $3P_{3/2}$ state of Na. The low-field F states are indicated, as are the m_J-labeled states at higher field values, where the **J** and **I** vectors decouple. AOC occurs in the transition region between these two limiting cases.

agonalizing the appropriate 16×16 Hamiltonian at each field value. Numerous level crossings occur in the 10–40 G region, and it is in this intermediate-coupled region that AOC is expected to attain a maximum.

The computed magnetic-field-dependent eigenstates and eigenenergies were used in Eq. (1) to calculate the expected degree of AOC. In the present experiment, we excite the atoms with linearly (z)-polarized light, and then observe the z-directed left and right circularly polarized (σ^+ and σ^-, respectively) fluorescence. Thus $f_{i\alpha}=\langle i|r^{(0)}|\alpha\rangle$ and $g^{\pm}_{j\beta}=\langle j|r^{(\pm)}|\beta\rangle$, where $r^{(0)}=z$ and $r^{(\pm)}=(x\pm iy)/\sqrt{2}$. The use of Eq. (1) then yields the circular-polarization fraction,

$$P_c=\frac{I_+-I_-}{I_++I_-}=\frac{R(f,g^+)-R(f,g^-)}{R(f,g^+)+R(f,g^-)}, \tag{2}$$

where I_+ (I_-) is the fluorescence intensity for σ^+ (σ^-) light. Spectrally-integrated $I_\pm$ values were calculated separately for $F'=1$ and 2, where each frequency range encompassed only excitation originating from the $3S_{1/2}F'=1$ or $F'=2$ hyperfine components (Fig. 3). The resulting P_c values are labeled P_c (F'), and the result using the entire spectral integration is labeled P_c (total).

III. EXPERIMENT

The fluorescence resulting from pulsed or steady-state white-light excitation is equivalent to the integrated fluorescence obtained by exciting the atoms with a scanning, monochromatic light source (having the same polarization). Thus, we have used a 1-MHz linewidth, cw dye laser to obtain the equivalent of white-light excitation. Furthermore, by integrating over the appropriate frequency ranges, we separate excitation to the Na $3P_{1/2}$ and $3P_{3/2}$ terms, as well as distinguishing between atoms initially in the $F'=1$ and $F'=2$ hyperfine levels of the $3S$ ground state.

The experimental setup is shown in Fig. 2. The Na atomic beam was produced by a recirculating oven; the Na density is discussed in Sec. IV. The homemade cw tunable ring dye laser was based upon a design by Hall, and had $a\sim1$ MHz linewidth that is much smaller than the natural transition linewidth of 10 Mhz and the residual beam Doppler width of ~15 MHz. The magnetic field was produced by two solenoids wrapped about 78-mm-long molybdenum yokes. The solenoids were separated from each other by $\simeq8$ mm. Each solenoid had a 10-μm inner and 19-mm outer diameter. The field in the approximately $0.5\times0.5\times1$ mm^3 volume defined by the intersection of the laser beam with the atomic beam had an estimated homogeneity of $\pm1\%$. The circular-polarization analyzer consisted of a $\lambda/4$ plate and a linear polarizer; the latter is rotated by 90° to pass the circular polarization of the opposite helicity. The polarization selectivity of the circular analyzer was measured to be greater than 99.8%.

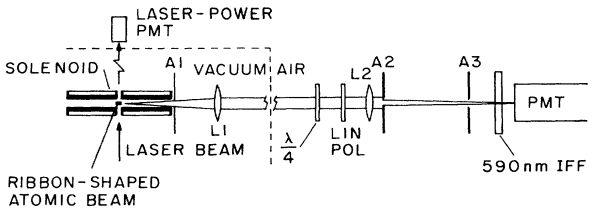

FIG. 2. A schematic plan view of the apparatus, as discussed in the text. Diameters of $A1$, $A2$, and $A3$ are 0.48, 0.76, and $\simeq0.1$ cm, respectively. Focal lengths of $L1$ and $L2$ are 15 and 10 cm, respectively. The vertical scale is expanded by a factor of 2 for clarity.

Two lenses (L_1,L_2) and three apertures (A_1,A_2,A_3) were used in the detection optics: A_1 served to block some of the instrumentally reflected light, L_1 collimated the detected fluorescence so that the light was normally incident on the circular polarization analyzer, L_2 imaged the source-region fluorescence onto A_3 (which was larger than the image of the fluorescence source but small enough to cut off most scattered laser light), and A_2 fixed the detected fluorescence solid angle. Preliminary data were collected with different A_2 diameters to ensure that the $\simeq0.8°$ (full angle) cone used during final data taking was sufficiently small that no correction to the observed circular polarization was needed. An interference filter (IFF) was placed after A_3 to reject extraneous light. A second photomultiplier monitored the laser power transmitted through the atomic beam.

Coils were installed outside the vacuum chamber (not shown in the figure) to null the earth's field in the x and y directions to within the $\simeq20$-mG sensitivity of our commercial gaussmeter. A small residual magnetic field in the z direction was compensated with a small offset current in the solenoids, chosen so that no AOC was detectable at 0 G.

The data-taking process was automated: a laboratory computer stepped the dye laser across the ~3 GHz scan range in 600 or 900 discrete frequency steps. These 3–5 MHz steps were 10–20% of the ~25 MHz residual Doppler plus natural linewidth. At each frequency, photon pulses were counted consecutively for the two circular polarizations and recorded by a data-acquisition system. Such scans were taken at a number of magnetic-field values between 0 and 80 G. For most magnetic-field strengths, scans were performed in consecutive pairs, one with the laser frequency increasing and the other with it decreasing, in order that any small, presumably linear, change in the atomic-beam density could be averaged away. The frequency linearity of the laser scan was monitored with an external reference cavity, and the ($<7\%$) nonlinearities were largely corrected in the subsequent data reduction.

The laser intensity was kept sufficiently low that optical pumping of the atoms during their transit time through the light field was insignificant. Several scans were taken at different intensities to confirm that the net circular polarization produced was independent of laser power.

IV. RESULTS AND DISCUSSION

Figure 3 illustrates the signals measured during a typical scan. The signal observed when the circular-

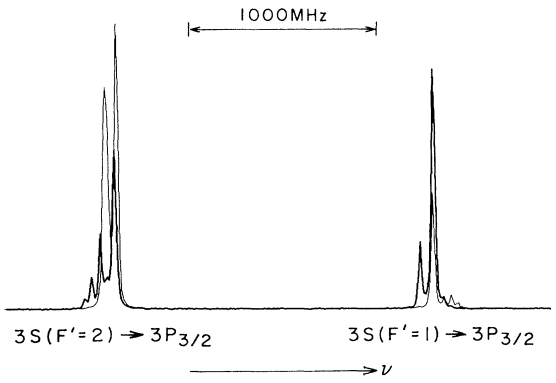

FIG. 3. A laser frequency scan, for a field of 23.6 G and with $\simeq 1$ s integration time per data point. The heavy and thin traces correspond to left and right circularly polarized fluorescence, respectively.

polarization analyzer passed only left-circular photons is shown with a heavy trace; the right-circular case is shown using a thinner trace. Although AOC here is a consequence of processes occurring in the ($P_{3/2}$) excited state, the clear resolution of the $3S_{1/2}$ $F'=1$ and $F'=2$ ground states (separated by 1772 MHz in zero field) allows one to separately measure the net circular polarization resulting from initial excitation from each of these two ground hyperfine states. However, before the area under the traces is evaluated to extract the net circular polarization, two corrections must be made to the data.

The first correction takes into account frequency-dependent variations in the exciting laser-beam intensity. One contribution to this variation was an etalon effect produced by the uncoated surface of the fused-silica vacuum-chamber window through which the laser beam entered. The laser-power-monitoring photomuliplier (PMT) detected this and was used to correct for it. To prevent a similar effect from the exit window, a glass wedge was attached to its inside surface with optical cement.

Another source of an intensity variation was the frequency-dependent absorption of the laser radiation as it passed through the atomic beam. Denoting the laser intensity before and after the atomic beam as I_0 and I_f, respectively, the average laser-beam intensity seen by the atoms is given by

$$I_{\rm av}=\frac{I_0(1-I_f/I_0)}{\ln(I_0/I_f)}\cong\frac{I_0+I_f}{2}\ . \tag{3}$$

I_f/I_0 was determined by measuring the dip in the signal of the laser-power PMT as the laser frequency was scanned across the transitions (Fig. 3). The minimum value of I_f/I_0 was ~ 0.94, and the effect of this partial absorption was corrected by dividing the signal by this average intensity. The corresponding Na column density is $\sim 3\times 10^8$ cm^{-2}.

The fluorescence can also be reabsorbed by a similar ($\sim 5\%$ maximum) amount. This fluorescence reabsorption probability is relatively independent of atomic beam width due to the different Doppler shifts of different beam regions. This absorption will attenuate the detected fluorescence, but it will do so by comparable amounts for both circular polarizations. Thus, after frequency integration this is expected to cause $<1\%$ uncertainty in the individual-F polarization data and less in the F-averaged data.

The second correction to the data takes into account the nonideality of the circular-polarization analysis system. Such deviations could be caused, for example, by imperfections in the quarter-wave plate or linear-polarization analyzer, residual birefringence in the output window, and depolarization due to scattered light. In order to quantify this effect, the magnetic field in the z direction was increased to $\cong 160$ G, a value where the individual $3S_{1/2}(F,m_F)$-$3P_{3/2}(m_J)$ transitions are clearly resolvable. The laser-beam polarization was rotated to be perpendicular to the magnetic-field direction, and the laser tuned to an isolated $\Delta m_J=+1$ or -1 transition for which the resulting fluorescence is known to be purely σ^+ or σ^-. (Recall it is not possible to excite $\Delta m=\pm 1$ transitions with light linearly polarized along the quantization axis.) The deviation of the measured polarization from pure circular polarization was then used to calibrate the optical system. This correction was in any case fairly small, leading to a less than 5% adjustment of the AOC data.

Figure 4 represents the measured (symbols) and calculated (solid line) P_c (total), P_C ($F'=1$), and P_c ($F'=2$) versus applied axial magnetic field. Also shown are calculated results assuming an infinite ground-state hyperfine constant (dashed lines), i.e., assuming that the ground state remains well described by the F,m_F representation independent of field strength. Under such circumstances, the observed circular polarization would be due entirely to excited-state AOC. Since the solid and dashed lines do not differ substantially, most of the net polarization is attributable to excited-state AOC, even at the highest magnetic fields presented in this figure.

Each measured point in Fig. 4 is an average of several scans. Since there were, in general, a differing number of

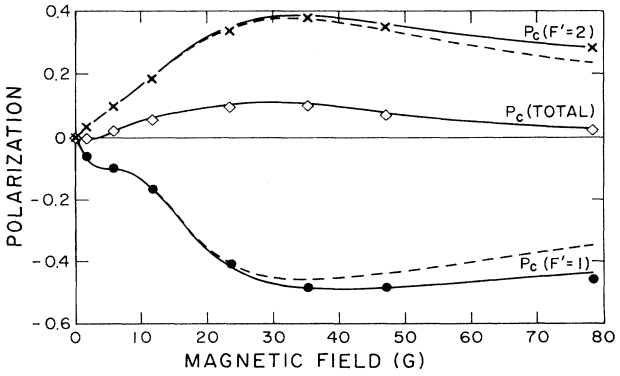

FIG. 4. Theoretical and measured circular-polarization fractions P_c. The dashed lines are the polarizations calculated using an infinite $3S_{1/2}$ hyperfine constant.

scans taken at each field strength, the random uncertainties are deduced by considering the scatter in the polarizations measured at 23.6 G, the value at which the largest number (17) of scans were performed. Half of the measured values fell within an absolute polarization range of about $\pm 0.8\%$, 1.2%, and 0.7% for P_c (total), P_c ($F'=1$), and P_c ($F'=2$), respectively. The statistical spread in the polarizations at the other magnetic-field strengths are consistent with these uncertainties.

The overall agreement between theory and experiment is striking. AOC attains a maximum of $\sim 8\%$ in the total polarization at approximately 30 G, and excitation from the individual ground-state hyperfine components produces large polarizations with different signs. Z-polarized white-light excitation would yield the P_c (total) result with fluorescence from the $3P_{3/2}$ state, and $\frac{2}{3}$ of this for the unresolved doublet. The AOC effect is expected to be generally less pronounced if charged particles rather than photons are used in the excitation process, since charged-particle collisions do not exclusively excite $\Delta m_L = 0$ transitions (except at threshold).

At small magnetic-field values, $|P_c\ (F'=1)|$ increases more rapidly than $|P_c\ (F'=2)|$. This is attributable to the smaller splittings between the $3P_{3/2}$ $F=0$, 1, and 2 hyperfine levels that are excited from $F'=1$, compared with the splittings between $F=1$, 2, and 3. Since P_c $(F'=1)<0$, this produces a minor ($\sim 0.5\%$) negative dip in the total polarization at about 2 G. Our measurements are consistent with the presence of this dip.

Some of the data show small deviations from the calculations, generally with measured polarization magnitudes slightly less than those theoretically expected. Many of these discrepancies may be attributed to the small inhomogeneity of the magnetic field within the interaction volume.

It is of interest to repeat this experiment with optical excitation to the $3P_{1/2}$ term. We thus performed a limited number of scans with the z-polarized laser scanning across the $3S_{1/2}$-$3P_{1/2}$ transition, in the presence of an intermediate (23.6 G) magnetic field. No overall orientation was observed, consistent with the theoretical prohibition on alignment of a $J=\frac{1}{2}$ state. A slight ($\sim 1.5\%$) polarization was seen for transitions originating from the resolved $3S_{1/2}$ $F'=1$ and 2 hyperfine states, but this was expected because of the small degree of decoupling of these states in the magnetic field, as discussed above.

V. CONCLUSIONS

We have performed a detailed experimental verification of AOC. This has confirmed quantitatively, with high signal-to-noise ratio and accuracy, that circular polarization is produced following linearly polarized excitation by intermediate-coupled states in a magnetic field. This effect has been shown to be much larger when the excitation occurs from one of the two ground hyperfine states. In addition to conceptual insight, this could be important in experiments where, for instance, most of the atoms have been optically pumped without orientation ("hyperfine pumping") into one of these F' ground states. If some excitation process then were to occur in an intermediate magnetic field, the resulting emission along the field direction from any alignable excited state may exhibit a significant degree of circular polarization.

As noted by Baylis,[3] AOC may also be of use in the determination of hyperfine-structure constants for excited states by measuring the magnetic-field dependence of the net circular polarization. This could be particularly useful for levels with hyperfine splittings less than the natural linewidth. An advantage of such a technique is that it does not place stringent requirements upon laser linewidth, which needs to only be less than the lower-state hyperfine splitting.

As discussed earlier, one would expect to observe an exactly analogous effect if the magnetic-field strength were increased sufficiently that the excited-state angular momentum **J** started to decouple into **L** and **S**. Although this transition region in sodium takes place for field strengths not usually encountered under laboratory conditions, it may be of more practical importance for transitions in other elements characterized by a much smaller excited-state fine-structure splitting.

It should be emphasized that it is not necessary to use linearly polarized light to produce the initial excited-state alignment. Any nonisotropic excitation process can lead to alignment of the atoms. Thus directed collisions or unpolarized light propagating in one direction could also produce alignment, which would be converted to orientation in the presence of a magnetic field of the appropriate strength. It is the pseudovector (i.e., parity-violating) nature of a magnetic field that permits AOC to take place; reflection symmetry precludes AOC from occurring if an electric field were used instead.

The process investigated here clearly has many similarities to the conventional Hanle effect, where it is the linearity (rather than circularly) polarized fluorescence propagating parallel or perpendicular to the magnetic-field direction, which is monitored as a function of field strength.[10] Indeed, the same Breit formula describes both, and the overall fluorescence intensity observed in our experiment did vary with the applied magnetic field, as predicted by the Hanle effect.

ACKNOWLEDGMENTS

This work could not have been completed without the valuable comments, advice, and encouragement of Alan Gallagher. Financial support was provided by the U.S. Department of Energy, Division of Chemical Sciences, Office of Basic Energy Sciences.

*Present address: Dept. of Physics, University of Idaho, Moscow, ID 83843.
†Present address: MPB Technologies Inc., 1725 North Service Road, Trans-Canada Highway, Dorval, Quebec, Canada H9P 1J1.

[1]U. Fano and J. H. Macek, Rev. Mod. Phys. **45**, 553 (1973).
[2]J. C. Lehmann, J. Phys. (Paris) **25**, 809 (1964); Phys. Rev. **178**, 153 (1969).
[3]W. E. Baylis, Phys. Lett. **26A**, 414 (1968).
[4]J. C. Kemp, J. H. Macek, and F. W. Nehring, Astrophys. J. **278**, 863 (1984).
[5]M. Krainska-Miszczak, J. Phys. B **12**, 555 (1979); **12**, L205 (1979).
[6]K. L. Stricklett, D. J. Burns, and P. D. Burrow, Phys. Rev. A **36**, 5280 (1987).
[7]H. Avci and H.-P. Neitzke, J. Phys. B **22**, 495 (1989).
[8]P. A. Franken, Phys. Rev. **121**, 508 (1961).
[9]A. Gallagher, Ph.D. dissertation, Columbia University, 1964. See Eq. (19): a factor $[(\nu-\nu_{\alpha i}+i\Gamma/4\pi)^{-1}-(\nu-\nu_{\alpha j}-i\Gamma/4\pi)^{-1}]$ multiplies the right-hand expression in our Eq. (1), where ν is the laser frequency.
[10]A. Corney, *Atomic and Laser Spectroscopy* (Clarendon, Oxford, 1977).